The cervical nerves and foramina: local-coil MR imaging.

D L Daniels, J S Hyde, J B Kneeland, A Jesmanowicz, W Froncisz, T M Grist, P Pech, A L Williams and V M Haughton

AJNR Am J Neuroradiol 1986, 7 (1) 129-133
http://www.ajnr.org/content/7/1/129

The Cervical Nerves and Foramina: Local-Coil MR Imaging

David L. Daniels[1]
James S. Hyde
J. Bruce Kneeland
A. Jesmanowicz
W. Froncisz
Thomas M. Grist
Peter Pech
Alan L. Williams
Victor M. Haughton

A detailed study of the magnetic resonance (MR) appearance of the cervical nerves and neural foramina is presented. Using a "butterfly" local coil and a 1.5-T GE Signa MR system, the authors obtained 3-mm-thick axial, parasagittal, and 45° oblique MR images of the cervical neural foramina in four normal volunteers. For the oblique images, subjects were rotated 45° toward the right posterior oblique. Neural and vascular structures in the foramina were identified by correlation of the MR images with corresponding cryomicrotomic sections from four cadavers. The 45° oblique images were more useful than axial or parasagittal images for demonstrating anatomic relations in the neural foramina. MR imaging with local coils demonstrates the complex anatomy of cervical neural foramina in various planes.

The myelographic and computed tomographic (CT) evaluation of the cervical neural foramina is not optimal. Positive-contrast myelography carries the risk of undesirable side effects and imperfect sensitivity or specificity for root sheath lesions [1, 2]. The CT evaluation of cervical nerves may be difficult, especially at the C7–T1 level or in the presence of minor degenerative changes that narrow the foramen and obscure the fat [3]. Intrathecal or intravenous contrast enhancement has not improved the sensitivity of CT sufficiently to earn it wide acceptance [3, 4]. CT images reformatted in 45° oblique planes, which show anatomic relations optimally in the neural foramen [5], have less resolution than does direct axial CT.

Magnetic resonance (MR) imaging has the potential to demonstrate cervical nerves without osseous artifacts and in several planes. Because of the deficiencies of CT, the use of MR imaging in the clinical evaluation of cervical disk disease is anticipated. We describe the normal appearance of the neural foramina in local-coil MR images.

Materials and Methods

Cervical spine specimens were removed from four fresh-frozen cadavers, embedded in styrofoam boxes with carboxymethyl cellulose gel, and sectioned with a heavy-duty sledge cryomicrotome (LKB 2250, Gaithersburg, MD) in axial, parasagittal, or 45° oblique planes [6, 7]. The surfaces of the specimens were photographed as they were sectioned.

MR images were obtained with a GE Signa 1.5-T system and a modified loop-gap resonator [8–10] as the receiver coil. The loop-gap resonator had a two-loop, single-gap "butterfly" configuration (Hyde J, unpublished data). Four normal volunteers (age range, 25–35 years) without clinical evidence of cervical radiculopathy were recruited for imaging. Sagittal and axial images were used for localization. For axial and parasagittal images, the volunteers were positioned supine on the Signa table with the loop-gap resonator under the neck. For the oblique images they were rotated 45° toward the right posterior oblique so that their sagittal plane formed an angle of 45° with the surface of the coil and tabletop. Technical factors included a repetition time (TR) of 800 msec, an echo time (TE) of 25 msec, a 128 × 256 or 256 × 256 matrix (pixel sizes of 1.2 × 0.6 mm and 0.6 × 0.6 mm, respectively), a 16-cm field of view, two excitations, and a 3-mm slice thickness. Two volunteers also had parasagittal images with a TR of both 400 and 2500 msec.

Received February 22, 1985; accepted after revision August 5, 1985.

This work was supported in part by a grant from General Electric Medical Systems and by grant RR01008 from the National Institutes of Health.

[1] All authors: Department of Radiology, Medical College of Wisconsin, Froedtert Memorial Lutheran Hospital, 9200 W. Wisconsin Ave., Milwaukee, WI 53226. Address reprint requests to D. L. Daniels.

AJNR 7:129–133, January/February 1986
0195–6108/86/0701–0129

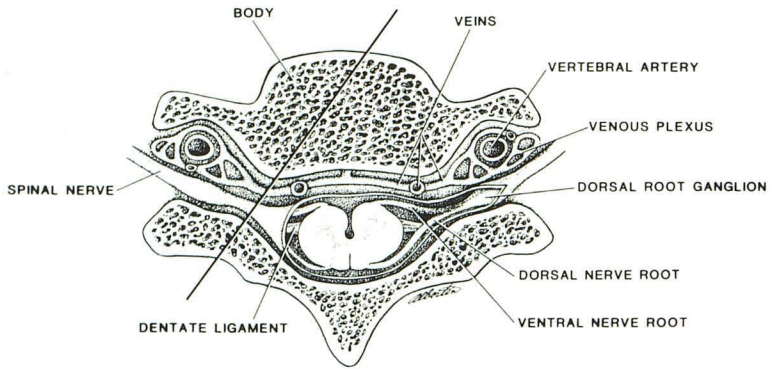

Fig. 1.—Cervical neural foramina in axial section. Intraforaminal veins are anterior to nerve roots and dorsal root ganglia; vertebral arteries are anterior to dorsal root ganglia. *Black line* represents plane of 45° oblique anatomic sections in fig. 5 and MR images in fig. 6. (Adapted from [4].)

Photographs of the cadaveric anatomic sections and the MR images of the volunteers were correlated to identify structures related to the cervical neural foramina including dorsal and ventral nerve roots, the dorsal root ganglion, small veins, and the vertebral artery (figs. 1–6).

Results and Discussion

Detailed anatomic descriptions of the cervical neural foramen have been published [7, 11]. The cervical nerve roots that form from the ventral and dorsal nerve rootlets on the cord surface extend anterolaterally at a 45° angle to the coronal plane and inferiorly at about 10° to the axial plane. The roots are located within the root sheath in the inferior half of the neural foramen (fig. 1). The dorsal nerve roots lie cranial and dorsal to the ventral nerve roots (figs. 4 and 5). The upper half of the neural foramen contains fat and small veins. The dorsal root ganglion lies outside the neural foramen between the vertebral artery and a small concavity in the superior articular process.

The MR appearance of the normal cervical foramen has not been described in detail. In local-coil MR images, structures that have a signal intensity intermediate between that of fat (high signal intensity) and that of cortical bone (negligible signal intensity) correspond in location and size to the dorsal and ventral nerve roots and dorsal root ganglia (figs. 2 and 3). The vertebral artery and small epidural veins are demonstrated because blood flowing in them produces negligible signal. The vertebral artery lies adjacent to the anterior surface of the ganglion. Small veins are shown in the anterocranial aspect of the foramina. In parasagittal and 45° oblique images, MR shows the cranial half of the foramen filled with fat (figs. 3 and 6) and small amounts of fat anterior to the nerve roots and dorsal root ganglion but little or no fat inferior and posterior to them. Foraminal fat is shown better with a longer TR (800 or 2500 msec) than with a shorter TR (400 msec) because the longer TR yields a better signal-to-noise ratio. The long-TR images are needed to define osteophytic ventral ridging and herniated disk in the sagittal plane [12–15].

The various MR imaging planes show different anatomic relations. The nerve roots, dorsal root ganglia, and vertebral artery are shown in axial, parasagittal, and 45° oblique planes. The 45° oblique plane is best for defining the contour of the cervical nerve roots and cervical foramina (pedicles cranially and caudally, uncinate process anteriorly, and superior and inferior articular processes of the adjacent vertebrae posteriorly) (fig. 6). In this plane, the uncinate process appears as a small, triangular osseous projection. Cortical bone surrounding the foramen has negligible signal, in contrast to foraminal fat (very high signal intensity) and medullary fat (high signal intensity) in the vertebral bodies, pedicles, and articular pillars. The axial and sagittal planes demonstrate the posterior margins of the disks; the sagittal plane demonstrates the spinal cord contour optimally.

MR imaging has several advantages over CT for evaluating cervical nerve roots. In one MR image, roots at several levels are demonstrated. Nerve roots, theoretically, can be demonstrated even when fat is replaced and foramina are narrowed. The visualization of the nerve roots with MR imaging appears to be at least as good as with CT. Local-coil design improvements may increase the anatomic detail in MR images. Therefore, MR imaging may provide a more effective, noninvasive tool for studying patients with radiculopathy. The oblique plane and the loop-gap resonator coils are likely to improve the MR detection of cervical herniated disks, which has been reported [12–15]. A clinical trial of MR imaging in cervical radiculopathy is planned.

REFERENCES

1. Strother CM. Cervical examination. In: Sackett JF, Strother CM, eds. *New techniques in myelography*. Hagerstown, MD: Harper & Row, **1979**
2. Fox AJ, Lin JP, Pinto RS, Kricheff II. Myelographic cervical nerve root deformities. *Radiology* **1975**;116:355–361
3. Daniels DL, Grogan JP, Johansen JG, Meyer GA, Williams AL,

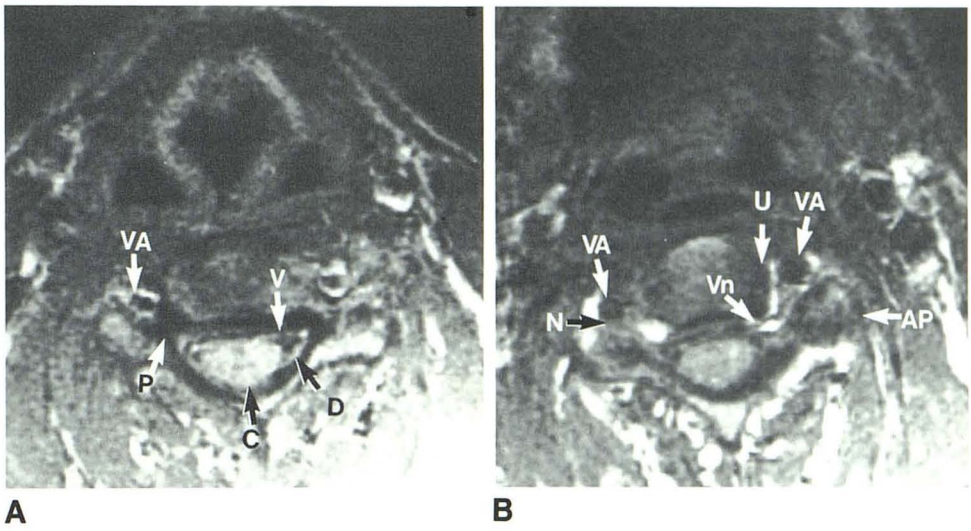

Fig. 2.—Axial MR images of cervical neural foramina. In **A**, the dorsal (D) and ventral (V) nerve roots are identified lateral to spinal cord (C). Vertebral artery (VA), with negligible signal, is anterolateral to pedicle (P). In **B**, slightly caudal to **A**, a vein (Vn) and a cervical nerve (N) are located at anterior and posterior aspects, respectively, of neural foramina. Fat in foramina has high signal intensity. Uncinate process (U) and articular pillar (AP) border neural foramen.

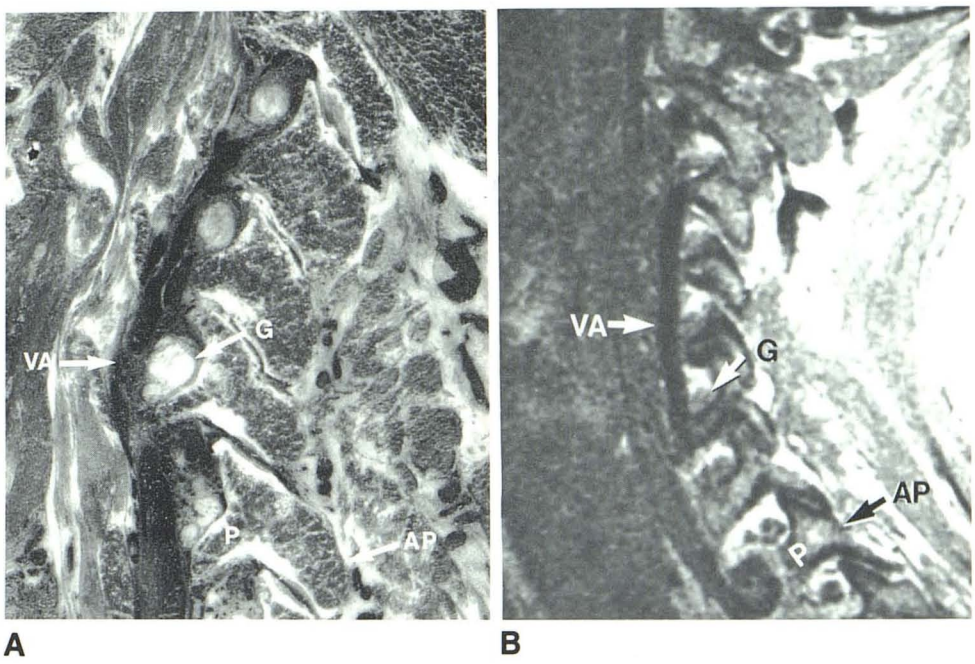

Fig. 3.—Correlative parasagittal anatomic section (**A**) and MR image (**B**) of dorsal root ganglion (G) lying posterior to vertebral artery (VA). P = pedicle; AP = articular pillar.

Haughton VM. Cervical radiculopathy: computed tomography and myelography compared. *Radiology* **1984**;151:109–113

4. Russell EJ, D'Angelo CM, Zimmerman RD, Czervionke LF, Huckman MS. Cervical disk herniation: CT demonstration after contrast enhancement. *Radiology* **1984**;152:703–712
5. Rauschning W, Rothman SLG. CT anatomy of the cervical spine in oblique reformatted planes. Presented at the annual meeting of the Radiologic Society of North America. Washington, DC: November **1984**
6. Rauschning W, Berstrom K, Pech P. Correlative craniospinal anatomy studies by computed tomography and cryomicrotomy. *J Comput Assist Tomogr* **1983**;7:9–13
7. Pech P, Daniels DL, Williams AL, Haughton VM. The cervical neural foramina: correlation of microtomy and CT anatomy. *Radiology* **1985**; 155:143–146
8. Froncisz W, Hyde JS. The loop-gap resonator: a new microwave lumped circuit ESR sample structure. *J Magnetic Resonance* **1982**;47:515–521
9. Wood RL, Froncisz W, Hyde JS. The loop-gap resonator II: controlled return flux three-loop, two-gap microwave resonators for ENDOR and ESR spectroscopy. *J Magnetic Resonance* **1984**;58:243–253
10. Grist TM, Hyde JS. Resonators for in-vivo ^{31}P NMR at 1–5 T. *J Magnetic Resonance* **1985**;61:571–578
11. Hadley LA. Intervertebral joint subluxation, bony impingement and foramen encroachment with nerve root changes. *AJR* **1951**;65:377–402
12. Modic MT, Weinstein MA, Paulicek W, Starnes DL, Duchesneau

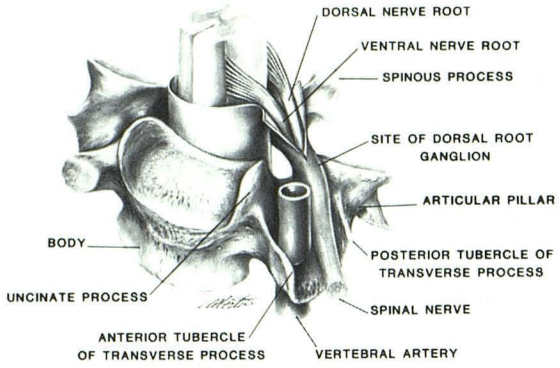

Fig. 4.—Cervical vertebra and spinal nerve as viewed from above and anterolaterally. Dorsal nerve root lies cranial and dorsal to ventral nerve root; dorsal root ganglion lies posterior to vertebral artery.

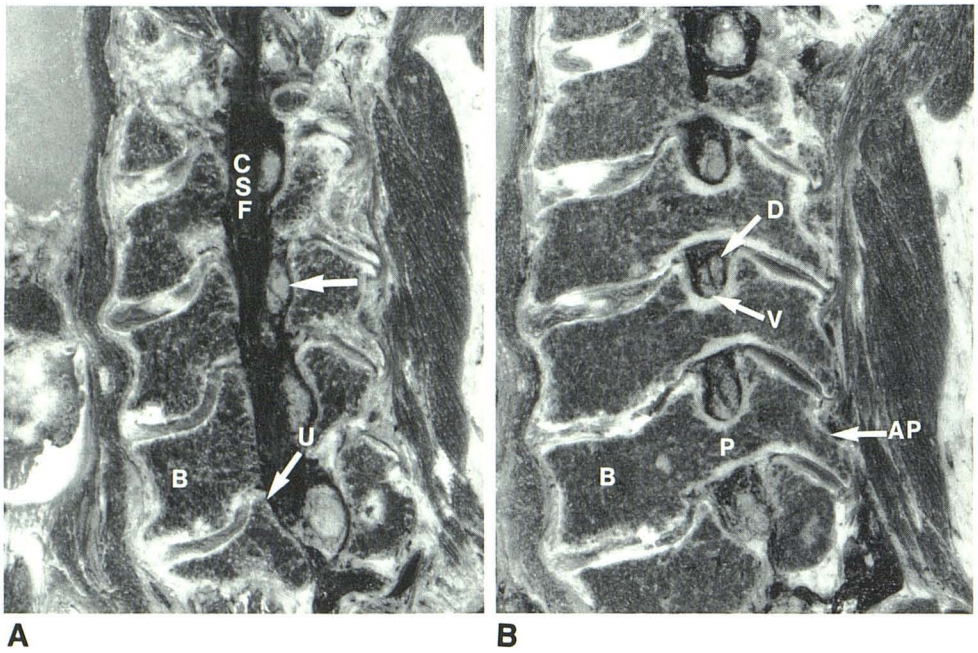

Fig. 5.—45° oblique anatomic sections. In medial slice (**A**), cerebrospinal fluid (CSF) is anterior to nerve roots (*larger arrow*). Uncinate process (U) appears as a triangular osseous projection. In lateral slice (**B**), dorsal (D) nerve roots are dorsal and cranial to ventral (V) nerve roots in neural foramina. Prominence of intraforaminal veins is due to postmortem changes. B = vertebral body; P = pedicle; AP = articular pillar.

PM, Boumphrey F, Hardy RJ Jr. Nuclear magnetic resonance imaging of the spine. *Radiology* **1983**;148:757–762

13. Han JS, Kaufman B, El Yousef SJ, et al. NMR imaging of the spine. *AJNR* **1983**;4:1151–1159, *AJR* **1983**;141:1137–1145
14. Norman D, Mills CM, Brant-Zawadzki M, Yeates A, Crooks LE, Kaufman L. Magnetic resonance imaging of the spinal cord and canal: potentials and limitations. *AJNR* **1984**;5:9–14, *AJR* **1983**;141:1147–1152
15. Modic MT, Weinstein MA, Pavlicek W, Boumphrey F, Starnes D, Duchesneau PM. Magnetic resonance imaging of the cervical spine: technical and clinical observations. *AJNR* **1984**;5:15–22, *AJR* **1983**;141:1129–1136

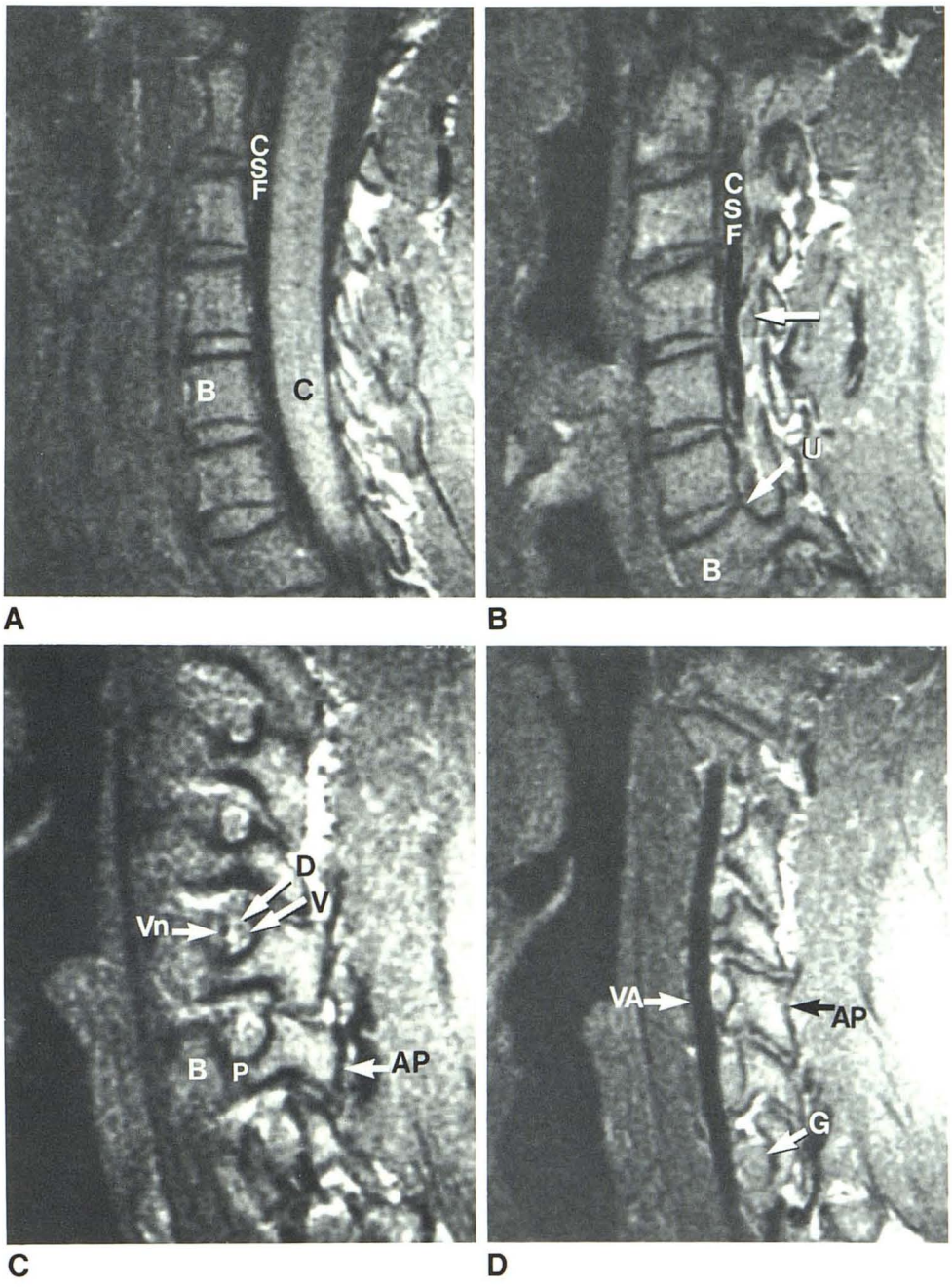

Fig. 6.—45° oblique MR images from medial (**A**) to lateral (**D**). In **A**, spinal cord (C) is displayed in contrast to cerebrospinal fluid (CSF), which has a negligible signal. B = vertebral body. In **B**, nerve roots (*upper arrow*) are distinguished from fat (high signal intensity) posterior to CSF. Uncinate process (U) of C7 is shown. In **C**, dorsal (D) and ventral (V) nerve roots and a vein (Vn) are demonstrated in cross section. Cortical bone in pedicles (P) and articular pillars (AP) has negligible signal. In **D**, a dorsal root ganglion (G) is identified posterior to vertebral artery (VA). **B** and **C** correspond to figs. 5A and 5B, respectively.